Thermal stability and degradation of a low refractive index photo-crosslinkable adhesive

Alexandre Godin, Clément Mailhé, Jérémy Barboure, Cédric Le Coz, Thomas Vidil, Abdelhak Saci, Sébastien Touzain, Marie Duquesne

Thermal stability and degradation of a low refractive index photo-crosslinkable adhesive

Alexandre Godin[1,2*], Clément Mailhé[3], Jérémy Barboure[4,5], Cédric Le Coz[5], Thomas Vidil[5], Abdelhak Saci[6], Sébastien Touzain[1], Marie Duquesne[1]

[1]*La Rochelle Université, LaSIE UMR CNRS 7356, Avenue Michel Crépeau, CEDEX 1, 17042 La Rochelle, France*
[2]*4ev Lab, EDF R&D, CNRS, LaSIE, La Rochelle University, Avenue Michel Crépeau, CEDEX 1, 17042 La Rochelle, France*
[3] *CNRS@CREATE Ltd., Create Tower, 1 Create Way #08-01, Singapore 138602,*
[4] *Bordeaux INP, CNRS, Université de Bordeaux I2M, Bât A11, 351 Cours de la Libération, 33400 Talence, France*
[5] *University Bordeaux, CNRS, Bordeaux INP, LCPO, UMR 5629, F-33600, Pessac, France*
[6] *Amplitude, 11 Avenue de Canteranne, Cité de la Photonique, Bâtiment MEROPA, 33600 Pessac, France*

* Corresponding author: alexandre.godin@univ-lr.fr

Abstract: In some laser assemblies, optical components are glued on their metal mount using a photocrosslinkable adhesive. All these components are submitted to medium to high temperatures for several hours upon laser's operation time. The subsequent thermal stresses endured by the adhesive could lead to its degradation, alter thus the functioning of the assembly and impact the alignment of the laser, key issues in laser applications. This work focuses on the investigation and the modeling of the lifespan, the degradation in the face of thermal stresses, particularly those generated by a laser, and of the ageing of a photocrosslinkable adhesive, PC373HA. The thermal characterization is performed using ThermoGravimetric Analysis and allows for the development, the validation and the comparison of three models based on Arrhenius' law to estimate the lifetime of adhesives as a function of temperature. A temperature of 150°C is identified as a threshold to ensure limited degradation over the 15 hours requested for laser operation endurances. The Ozawa-Flynn-Wall model and the Kissinger-Akahira-Sunose model correctly reproduce PC373HA's thermal behavior submitted to different thermal scenarii (temperatures, heating rates…). Both show that the higher the temperature, the faster the degradation process, approximately 10 minutes at 220°C and 100 minutes at 180°C, much less than the required 15 hours. Besides, in the event of an incident with the laser, if the temperature exceeds 200°C for more than 10 minutes or 180°C for more than 100 minutes, corrective action should be taken, and the adhesive should be replaced. These models therefore provide fundamental information for laser applications and will allow the implementation of preventive solutions during use but also in case of incident.

Keywords: UV curing; Degradation modeling; TGA; Thermal degradation

1. Introduction

Adhesives are polymers used to bind surfaces of identical or different natures. Practical applications of these materials can be found in a vast number of industries which explains their appeal in research. Their interest originates from the range of their properties which make their use tailorable to a number of contexts based on mechanical considerations [1-5], thermal considerations [6], practical considerations [7] or a combination of them.

During service, polymers are aged by environmental factors (UV, temperature, oxygen, water…) which implies a change in their properties. Physical ageing, as defined by Struik [8-10], is a natural evolution of the polymer network below the glass transition temperature to recover an equilibrium state and is a reversible phenomenon. Chemical ageing is due to a chemical change of the polymer structure (reaction with oxygen and/or water, covalent bond breaking, …) and is an irreversible process leading to the polymer degradation. Specifically, thermal degradation occurs when temperature is high enough so primary chemical bonds are dissociated. This process typically arises at temperatures around 150-200°C and the degradation rate increases as the temperature increases [11].

In some laser assemblies, optical components (glass or crystal) are glued on their metal mount with photocrosslinkable adhesives. The laser assembly (metal, crystal and adhesives) can endure temperatures up to 220°C during its use which can lead to the thermal degradation of the adhesive. Therefore, the component degradation (partial or total) would alter the functioning of the assembly, key issues in laser applications. Indeed, this could misalign the laser and have serious consequences (for instance in laser applications such as ophthalmology, brazing etc.). Several works have been carried out on the characterization of adhesives used in laser applications [12-19] but none on the lifespan of these adhesives, their degradation under thermal stresses, particularly those generated by a laser, and on the ageing of these adhesives.

This work focuses on the study of these latter issues, crucial to ensure the proper functioning of the laser and the associated assembly investigating the thermal behavior of a currently used commercially available adhesive, the PC373HA from Luvantix ADM. Very limited data is available from the supplier in order to estimate the lifespan of the adhesive under specific conditions, despite its widespread use in optical applications. Herein, the thermo-oxidative degradation of this adhesive is studied through accelerated ageing using thermogravimetric analysis in static isothermal experiments at different temperatures and in dynamic experiments at different heating rates for the duration of the requested laser operation endurances including stabilization time (approximately 15 hours in total). Experimental results are used to build three models, to validate and to compare them as well as extrapolate the life expectancy of the adhesives based on a mass loss criterion of degradation through different scenarii (i.e operating conditions: temperatures, heating rates…). This study is the first to demonstrate that conventional low-refractive index acrylic adhesives have limited thermal stability at temperatures above 150 °C. Given that these temperatures can be reached, particularly in situations involving incidental laser beam exposure, this finding is critical for the safe and effective use of these adhesives. The practical implications of these results are twofold: (i) to prevent the use of these adhesives in applications where repeated high-temperature exposure occurs, and (ii) to implement preventive measures, such as adhesive replacement, in cases of unexpected overheating.

2. Materials

The PC373HA is a radiation-curable acrylate adhesive, commonly employed in fiber optics applications (Figure 1) due to its “cladding” optical properties that plays an active role in guiding the wave [20]. The adhesive hence needs a lower refractive index in comparison with the fiber one. Due to the increasing power of lasers, satisfying performances of the adhesives must be ensured in a wide range of temperatures usually ranging from 0°C to 220°C encompassing temperatures that can be met by the

laser apparatus during its use. Although commercially available, the PC373HA degradation, lifespan and ageing do not appear to have ever been characterized in the literature. Figure 8 in Annex shows the dynamic mechanical analysis (DMA) for a rectangular specimen of photo-crosslinked PC373HA (3-point bending, deformation ε = 5 μm, frequency f = 1 Hz). The peak maximum of the tan(δ) curve was used as the determination criterion for the glass transition temperature for the PC373HA adhesive and the value T_g = 52 °C was obtained. Comparing with data given by the manufacturer T_g = 73 °C, the difference is 20 °C. In view of these first results, it is important to know how long this adhesive will last under operating conditions.

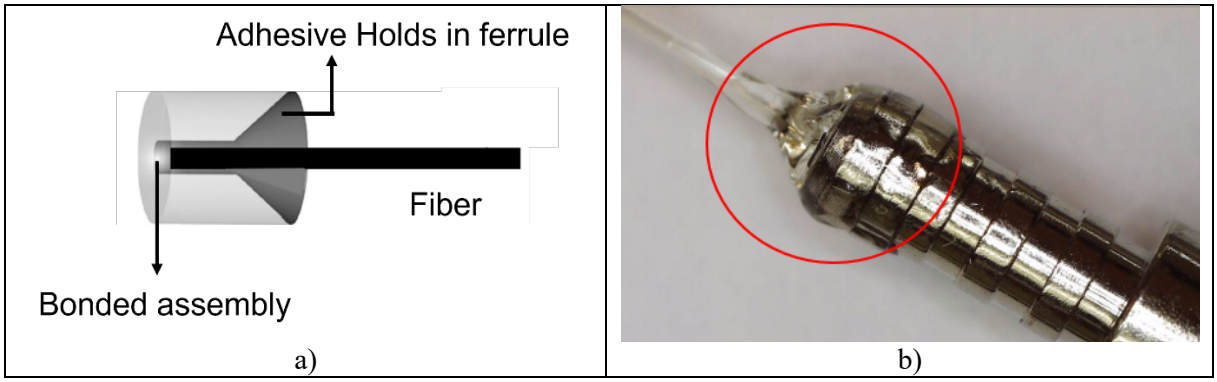

Figure 1. a) Sketch of the application for the adhesive; b) Assembly where the PC373HA is use.

The conservation period of photo-crosslinkable adhesives is relatively short with on average six months at ambient temperature (between 15 and 25 °C) and sheltered from light exposure due to its high reactivity [21]. The crosslinked adhesive samples used for the thermal characterization have been obtained by photo-polymerization in a AUV Cure oven equipped with a lamp consisting of an array of 365 nm UV LEDs with a total power of 200W. An average exposure of 1 min at 100% power has been applied for the photo-crosslinking process. Figure 9 in Annex represents the Infrared spectra of the resin before and after exposure to UV. The adsorption band at 1640 cm^{-1} and 1730 cm^{-1} are consistent with the vibrations of the C=O and the C=C double bonds of the acrylate functions respectively. They confirm that PC373HA is an acrylate adhesive. The total disappearance of the band corresponding to the C=C double bonds after UV exposure is consistent with the efficient photo-crosslinking of the adhesive.

3. Degradation modeling and thermal characterization

3.1 Degradation modeling

The assessment of the lifespan of adhesives at medium to high temperatures is essential. It consists in evaluating the period during which the material properties remain within acceptable limits. The properties of the materials are continuously altered throughout their use and it is assumed that a it is no longer viable after a 5% mass loss threshold [22-23]. The estimation of the lifespan of polymeric adhesives by accelerated ageing is an essential tool for both qualitative and quantitative comparisons. This is achieved by modeling the degradation process and validating it against experimental data collected during accelerated degradation experiments.

An important aspect of the modeling of the degradation process is the kinetic description that consists in estimating the activation energy (E_a $(J.mol^{-1})$), the Arrhenius pre-exponential factor (A (min^{-1})) and the order of the reaction (n). These parameters are of theoretical and practical significance, but require a solid understanding of the chemical reaction mechanisms that occur during thermal degradation. For non-isothermal experiments, the extent of the polymer degradation is assessed through mass loss monitoring. The mass loss rate increases with temperature reflecting the progress of the

degradation extent. An increase in the temperature usually leads to an increase in the degradation kinetics associated with an increase of the kinetic rate constant $\left(k(T)\ \ (min^{-1})\right)$. The relation between the kinetic rate constant and the temperature is described by the Arrhenius equation (Equation 1).

$$k(T) = Ae^{\frac{E_a}{RT}} \tag{1}$$

with R the gas constant (8.314 J mol^{-1} K^{-1}) and T the absolute temperature (K) of the adhesive.

A derived form of the Arrhenius law linking the degradation time t_i to the activation energy, the absolute temperature, T, and a dimensionless parameter B can be expressed as in Equation 2.

$$ln\ (t_i)\ =\ \frac{E_a}{RT} + B \tag{2}$$

The experimental results of the thermogravimetric analysis (described in the following subsection) allow modeling the lifespan of the adhesive using the Arrhenius law. For that, one first needs to verify that the $ln\ (t_i)\ =\ f(\frac{1}{T})$ curves are linear for a given degradation extent, α, considered as the mass loss criterion (*i.e.* the mass loss percentage considered as the threshold level of the degradation progress). α is defined as $(m_{init.} - m_{t_i})/m_{init.}$ where $m_{init.}$ is the initial mass of the sample and m_{t_i} is the mass of samples at time t_i during thermal degradation at the temperature T.

Equation 2 enables the estimation of a polymer's lifespan at a specific temperature based on accelerated aging experiments conducted at elevated temperatures. However, this approach relies on several key assumptions. The Arrhenius law, while widely applied, does not account for potential variations in activation energy throughout the degradation process. Specifically, the Arrhenius model presumes that the degradation mechanisms remain consistent across all temperatures, including both high testing temperatures and actual use temperatures – a condition that is often unrealistic. In reality, degradation mechanisms can differ significantly at lower temperatures. Furthermore, even at a constant temperature, the degradation mechanism may evolve as degradation progresses (*i.e.*, as a function of the degradation extent, α). The Arrhenius model does not incorporate these possible variations, which limits its reliability for extrapolating polymer lifespan solely based on a linear relationship between time and temperature as in Equation 2. To address these limitations, it is essential to apply one of the activation energy estimation models introduced below, which allow for the evaluation of the activation energy, E_a, as a function of degradation extent α, during accelerated aging experiments performed at different heating rates.

Three model are tested in this work, including two integration models that do not require any additional assumptions: the Ozawa-Flynn-Wall model (OFW, Equation 3, [24]) and the Kissinger-Akahira-Sunose model (KAS, Equation 4, [24]).

$$ln\ (\beta_i)\ \approx ln\left(\frac{A_\alpha E_\alpha}{R}\right) - ln\left(g(\alpha)\right)\ - 5.3305 - 1.052\left(\frac{E_\alpha}{RT_{\alpha,i}}\right) \tag{3}$$

$$ln\left(\frac{\beta_i}{T_{\alpha,i}^2}\right) \approx ln\left(\frac{A_\alpha R}{E_\alpha}\right) - ln\left(g(\alpha)\right) - \frac{E_\alpha}{RT_{\alpha,i}} \tag{4}$$

with β_i (°C.min^{-1}) the heating rate, α (%) the extent of the degradation process, R (J.K^{-1}.mol^{-1}) the universal gas constant, $T_{\alpha,i}$ (°C) the temperature for a given degradation extent, α, A_α (min^{-1}) the pre-exponential factor of the Arrhenius law and $g(\alpha)$ (%.min^{-1}) an integration term for $\frac{d\alpha}{dt}$.

These models are based on the isoconversion principle, a robust kinetics method for processing thermoanalytic data. They assume that the pre-exponential factor and activation energy do not depend on temperature, though they remain interdependent.

The models are used in experiments where the sample undergoes degradation during a temperature ramp at a specific heating rate, β_i. They relate the degradation extent α to the temperature $T_{\alpha,i}$. It is particularly adapted for systems with multiple reactions, accommodating variations in activation energy as degradation progresses with α. However, for simultaneous reactions of very different nature the OFW model is less applicable. The KAS model has been developed to overcome this limitation. This model, leveraging the Coats-Redfern approximation, is one of the most reliable isoconversional methods and does not require prior knowledge of the specific thermal degradation mechanism [25].

Both model enable the estimation of the activation energy, E_α, for the degradation reaction. This is achieved by respectively plotting $ln\ (\beta_i)\ = f\left(\frac{1}{T_{\alpha,i}}\right)$ and $ln\ \left(\frac{\beta_i}{{T_{\alpha,i}}^2}\right)\ = f\left(\frac{1}{T_{\alpha,i}}\right)$, for a given value of α. The plots should yield linear curves with slopes proportional to $\frac{E_\alpha}{R}$.

Those two similar models are also compared to a third isoconversional differential one called Friedman model (FR, Equation 5, [26]).

$$\frac{d\alpha}{dt} = A.exp\left(-\frac{E_\alpha}{R.T}\right).f(\alpha) \tag{5}$$

where $f(\alpha)$ (%.min^{-1}) is an integration term for $\frac{d\alpha}{dt}$.

In this case, it is possible to estimate the effective activation energy, E_α, by plotting $ln\ \left(\frac{d\alpha}{dt}\right)\ = f(\frac{1}{T})$ for several heating rates, β_i, according to the same principle than for the previous models.

The main advantages of the isoconversional methods are their ability to determine the effective activation energy E_α with no assumptions regarding the mechanism of degradation. A change in E_α can usually be explained by modification of the degradation mechanism or in the extent to which reaction rate limitations affect the process, as measured by thermoanalytic techniques. The isoconversional methods require a series of experiments at different heating ramps, β_i, and the estimation of the effective activation energy at different degradation extent, α. A significant variation of the activation energy according to α implies a kinetically complex process. In such cases, understanding how activation energy depends on α provides valuable mechanistic and kinetic insights, offering a clearer view of the multi-step degradation process and enabling more reliable predictions of its kinetics. A series of thermogravimetric analyses has therefore been performed to build and validate the latter models in the case of the low refractive index photo-crosslinkable adhesive PC373HA.

3.2 Thermogravimetric analysis

The ageing of material in typical operational conditions can be time consuming if noticeable changes are to be witnessed. A characterization is therefore required to study the degradation process and assess the lifespan of crosslinked adhesives. On the basis of accelerated ageing experiments, an estimation of the resistance to ageing of the studied adhesive is obtained. The rate of chemical reaction usually increases with temperature. This phenomenon is exploited for the study of accelerated ageing.

Amongst thermal analysis methods, the thermogravimetric analysis (TGA) is the most commonly employed for the study of materials degradation in terms of mass loss [27-32]. This method enable the precise monitoring of the sample mass according to temperature and time, and thus the assessment of

thermodynamic and kinetic parameters related to the degradation reaction responsible for the mass loss. By submitting the samples to high temperatures, it is possible to monitor the evolution of the degradation extent, α, as a function of temperature. It is then possible, through extrapolation, to predict the time dependence of α for any degradation temperature.

The thermal degradation experiments have been performed with a TA Q500 TGA apparatus with an airflow rate of 60 mL/min [33]. The adhesive sample is polymerized in a 400 µL aluminum crucible placed on a platinum platform of the TGA apparatus. The target mass is around 10 mg. The preparation of each sample is made using a METTLER TOLEDO weighing scale with a 0.03 mg uncertainty. The duration of the laser operation including the required stabilization time is about 15 hours (or 900 minutes). In order to allow for a margin, we carry out all our experiments over a period of 1000 min.

First, isothermal experiments are performed at temperature ranging from 50 °C to 220 °C to simulate the operating conditions of the laser but also to assess the operational limits of the adhesives assuming a 5% mass loss degradation criterion (α = 5%). The results are presented in Figure 2.

Besides, it is crucial to estimate the temperature limit for long term use according to different thermal scenarii that the adhesive may undergo. The Arrhenius law (Equation 2) must then be used to extrapolate the isothermal curves from Figure 2. However, it must first be verified that the activation energy remains constant throughout the degradation process. In order to verify this aspect, TGA experiments at different heating rates (2, 4, 6, 8 and 10 °C min^{-1}) are performed [34]. As 600 °C is the maximum recommended temperature for the used aluminum crucibles, samples are submitted to temperature raises from ambient temperatures to 600°C.

A summary of the tests carried out is available in Table 1.

Table 1. Summary of the thermal degradation experiments for 10 mg-samples of PC373HA over 1000 minutes.

Isothermal experiments	Temperatures T (°C)	50 70 120 150 180 200 220
Heating ramps, 20 °C to 600 °C	Heating rates β (°C.min^{-1})	2 4 6 8 10

4 Results & Discussion

All measured temperatures are expressed in degrees Celsius (°C) whereas all modeled temperatures are expressed in degrees Kelvin (K).

4.1 Experimental study of the thermal degradation

Isothermal TGA experiments at different temperatures allow for the observation of the behavior of the adhesives while the laser is operational. Figure 1 shows the isothermal curves at 70, 120, 150, 180, 200 and 220°C for the PC373HA. For T = 150 °C, the experiment was repeated twice (Annex, Figure 9). The replicates suggest that the temperature corresponding to a 5% mass loss can be determined with a precision of approximately ± 15 min.

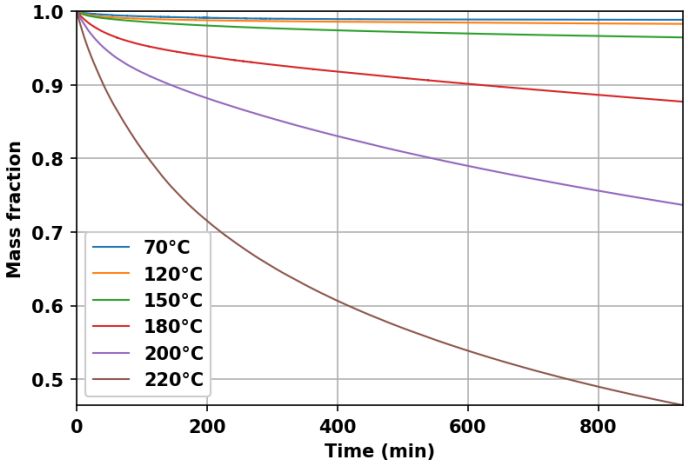

Figure 2. PC373HA isothermal TGA curves for a duration of 1000 minutes with an airflow rate of 60mL/min.

It can be noticed that the degradation rate increases significantly when the temperature of the isotherm is increased from 150 °C and 180 °C. Indeed, for isothermals below 150 °C, the mass loss barely reaches 3% while the 5% mass loss degradation threshold appears to be met at higher temperatures. This observation shows that 150 °C should be considered as a limit temperature for the operating conditions of the PC373HA from a purely thermal aspect.

The results of the dynamic experiments with heating rates β_i ranging from 2 and 10 °C.min^{-1} are presented in Figure 3 to assess the lifespan of the adhesive according to temperature for a mass loss criterion of 5%. For all heating rates (except 4 °C.min^{-1}), the experiments were repeated twice. The two curves recorded for β_i = 2 °C.min^{-1} are represented in the Annex (Figure 10). The replicates indicate a very good consistency of the data.

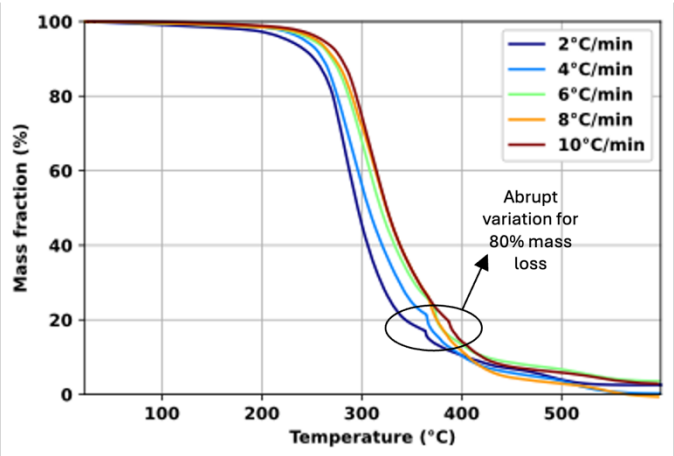

Figure 3. PC373HA TGA curves at different heating rates with a 60mL/min airflow rate.

These experiments show that the degradation process is shifted towards lower temperatures as the heating rate decreases. It can also be noticed that for all heating rates, the kinetics of degradation changes abruptly around 80% of mass loss (indicated by an arrow on Figure 3). Since this phenomenon appears

to be relatively independent of temperature (between 350°C and 400°C) or heating rate (between 2 and 10°C min^{-1}), it is likely that a significant change in structure or chemical composition is occurring at this time.

To observe this phenomenon more closely, Figure 4 represents the evolution of the mass fraction as a function of time (blue curve) for a PC373HA sample submitted to a 2 °C.min^{-1} heating rate, as well as the first derivative of the mass fraction with respect to time (red curve). This figure clearly shows two distinct steps of degradation. A first one, very broad, occurring between 260°C and 360°C and a second one marked by an abrupt mass loss at ~ 370 °C (clearly indicated by a sharp peak on the red curve). This second degradation stage might be related to the formation of oxidized products, which are entirely different from the product of the main degradation stage [35]. Unfortunately, it was not possible to analyze these residues by spectrometric analyses, due to the very low amount of material that is available at this stage of the experiment.

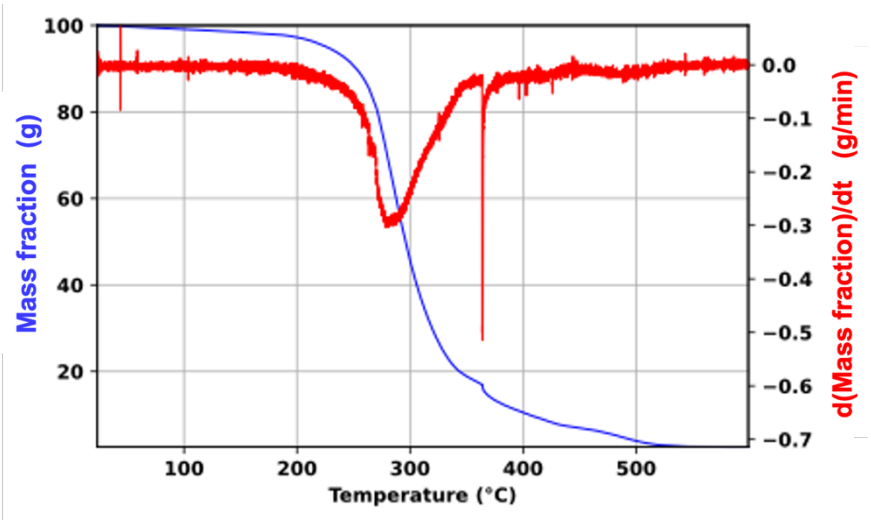

Figure 4. TGA curves for the PC373HA representing the evolution of the mass loss (blue) and the rate of mass loss (red) for a heating rate of 2°C/min and with airflow rate of 60mL/min.

4.2 Degradation modeling

The evolution of the activation energy, E_α, as a function of the degradation extent, α, can now be assessed for the three isoconversional methods KAS, OFW and FR [36]. We can plot $ln\ (\beta_i) = f\left(\frac{1}{T}\right)$, $ln\left(\frac{\beta_i}{T^2}\right) = f\left(\frac{1}{T}\right)$ and $ln\left(\frac{d\alpha}{dt}\right) = f(\frac{1}{T})$ for the OFW, KAS and FR models respectively using Equations 3, 4 and 5. The associated activation energies can then be estimated for different values of α.

Figure 5 shows the plots for α values ranging from 5% to 65% using KAS model. One can notice that the slope of the linear plots, i.e. E_α, varies with α thus suggesting that the degradation mechanism evolves during the process. It is also noticeable that the consistency between the linear regression and the experimental datapoints decreases for the highest values of α (> 25%). Figure 6 presents the evolution of the activation energy extracted from the slope of the plots of Figure 5, E_α, as a function of the mass loss, α. It is compared to the results obtained with the two other models, the OFW and the FR models, as well as with the Arrhenius law.

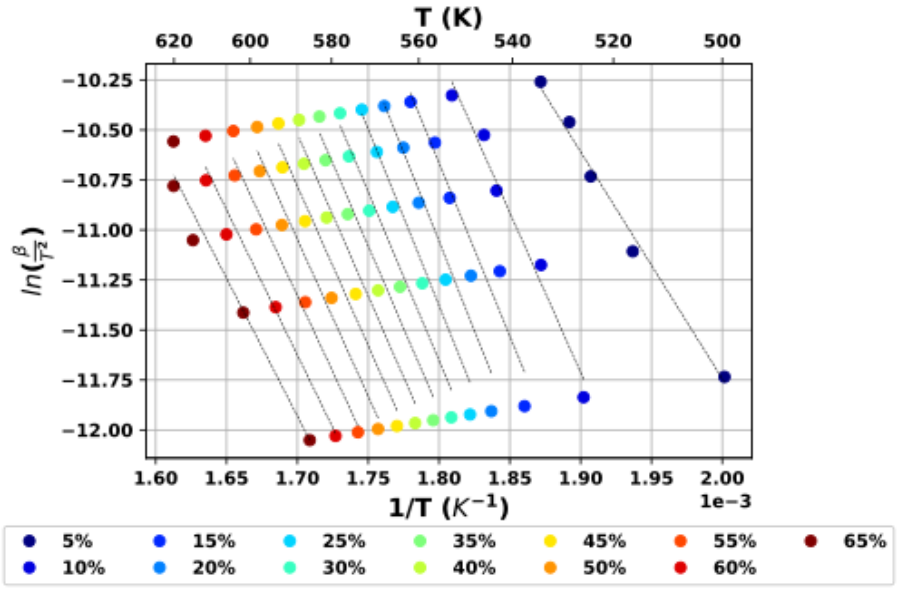

Figure 5. Arrhenius plots using KAS model for the PC373HA.

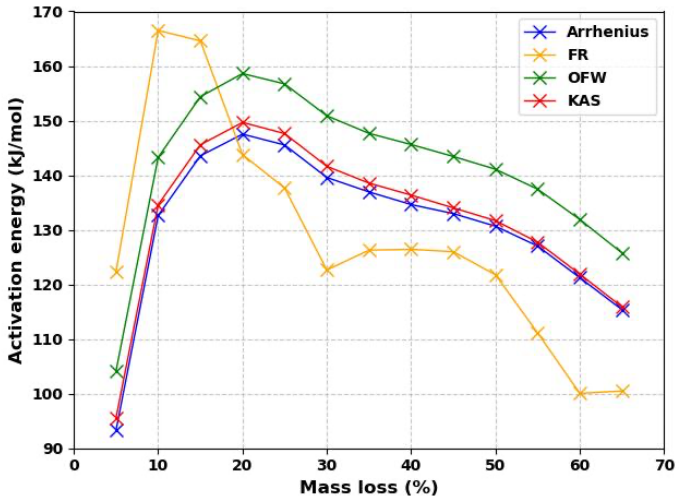

Figure 6. Activation energy as a function of PC373HA's degradation in terms of mass loss for the three isoconversional models and the Arrhenius law.

Table 2: Values of the Activation energy, E_a, as a function of the mass loss for the three isoconversional models and the Arrhenius law.

Mass loss (%)	Activation Energy, E_a (KJ.mol^{-1})			
	Arrhenius	FR model	OFW model	KAS model
5	93.30	122.34	104.16	95.55
10	132.64	166.50	143.28	134.60
15	143.55	164.60	154.37	145.57
20	147.52	143.77	158.61	149.67
25	145.53	137.65	156.71	147.62
30	139.58	122.64	150.87	141.62
35	136.94	126.28	147.66	138.55
40	134.62	126.42	145.62	136.36
45	132.97	125.99	143.43	134.02
50	130.66	121.76	141.09	131.68
55	127.02	111.12	137.44	127.73
60	121.23	100.05	131.89	121.88
65	115.38	100.49	125.76	115.88

Figure 6 shows that the activation energy varies with the mass loss. It indicates that the degradation process follows a complex mechanism, most certainly with several simultaneous reactions. For all models, a first step marked by a sharp increase in the activation energy is observed, likely due to the loss of the volatile compounds that are not covalently bonded to the crosslinked network of the adhesive. At later degradation stages, when only the crosslinked adhesive remains, the activation energy initially reaches a steady maximum, probably corresponding to the main degradation process. This is followed by a gradual decrease in activation energy, likely due to the combined effects of multiple phenomena: the primary degradation process, the progressive elimination of volatile compounds produced by this degradation, and the initiation of further secondary degradative reactions. It is noteworthy that the FR model yields slightly different results compared to the OFW and KAS models. All models, however, yield very similar trends, thus supporting the validity of the experimental approaches.

With these activation energies and the experimental isothermal curves shown in Figure 2, it is possible using Equation 2 to extrapolate PC373HA's lifespan. First the B parameter must be computed for the given degradation criterion, α = 5%, for all isothermals for which this criterion has been met (180, 200 and 220°C) and for each model. The parameter B is then chosen as the average value between the three temperatures (B_{avg}). The data regarding the calculation of this parameter and the corresponding standard deviations (σ) is given in Table 3.

Table 3. Determination of the B parameter of the Arrhenius equation for TGA isothermal experiments at 180, 200 and 220°C for the PC373HA.

Model	**E_a (kJ/mol)**	**B**			**B_{avg} (σ)**
		180°C	200°C	220°C	

KAS	95.62	-20.58	-20.56	-20.46	-20.54 (0.05)
OFW	104.20	-22.86	-22.74	-22.55	-22.72 (0.13)
FR	122.66	-27.76	-27.44	-27.06	-27.42 (0.29)
Arrhenius' law	93.57	-20.04	-20.05	-19.96	-20.01 (0.04)

Once the parameter B has been estimated, it is possible to plot the PC373HA's extrapolated lifespan for a mass loss criterion of 5% for each model. The curves are given in Figure 7.

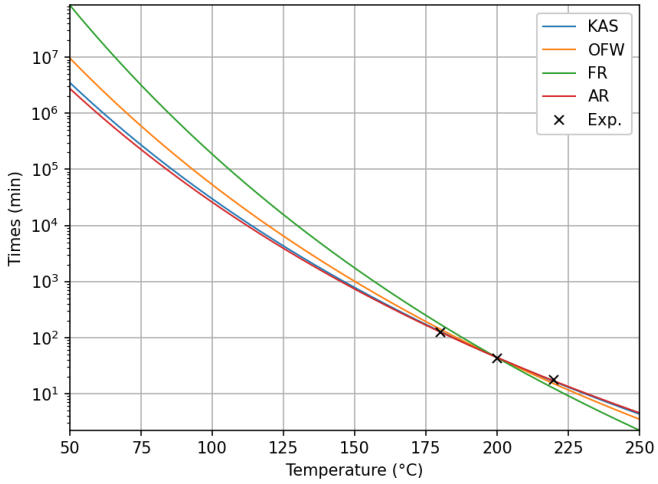

Figure 7. Extrapolated lifespan curves for each model for a mass loss criterion of 5%.

It appears that the Arrhenius standard model and the KAS model provide similar extrapolated lifespans over a wide temperature range and are consistent with the experimental data at 180, 200 and 220°C. The OFW model provides an acceptable approach with temperature range of the experimental data but drifts away from the Arrhenius law at low or high temperatures. On the other hand the FR modeling cannot give an acceptable estimation even within the temperature range of the isothermal TGA experiments. The KAS and OFW models indeed use data related to the advancement of the degradation assimilated to mass loss while the FR model uses the temporal derivative of the advancement assimilated to the rate of mass loss. If we observe the evolution of those two parameters in Figure 4, it can be noticed that the rate of mass loss (red) presents noise which could explain the unreliable results provided by the FR model.

KAS and OFW models correctly reproduce PC373HA's thermal behavior submitted to different thermal scenarii (temperatures, heating rates…). Both show that the higher the temperature, the faster the degradation process, approximately 10 minutes at 220°C and 100 minutes at 180°C, much less than the required 15 hours. It is therefore not recommended to use the PC373HA in laser applications where it is subjected to temperatures above 150°C. Also, in the event of an incident with the laser, if the temperature exceeds 200°C for more than 10 minutes or 180°C for more than 100 minutes, corrective action should be taken and the adhesive should be replaced.

This study allows to better anticipate the possible deteriorations during the use of a laser assembly or the damages due to the occurrence of an incident. It helps to consider the corrective actions necessary for an efficient functioning of the laser.

5 Conclusion

In this work, we investigate a commercial photocrosslinkable adhesive, PC373HA under thermo-oxidative conditions, and its application in laser equipment (in fiber optics applications). Due to the increasing power of lasers, satisfying performances of the adhesives must be ensured in a wide range of temperatures usually ranging from ambient to 220°C encompassing temperatures that can be met by the laser apparatus during its use.

Thermogravimetric analyses allowed the simulation of PC373HA's accelerated ageing. These analyses allowed the building of Arrhenius type models in order to estimate an activation energy for a 5% mass loss in TGA (chosen as criteria of the begining of the degradation process).

The Ozawa-Flynn-Wall model and the Kissinger-Akahira-Sunose model correctly reproduce PC373HA's thermal behavior submitted to temperatures ranging from 50°C to 220°C and heating rates ranging from 2°C.min^{-1} to 10°C min^{-1}. They show that the degradation process starts approximately after 10 minutes at 220°C and after 100 minutes at 180°C, much less than the required 15 hours for laser operation endurances. Some adhesives might withstand such severe conditions. They include polyimide or phenolic adhesives that can be used at service temperatures close to 200 °C [37]. However, their curing processes are complex and are not suitable for optic applications. 150°C is the limit temperature for PC373HA and it is therefore not recommended to use this low refractive index photocrosslinkable adhesive in laser applications where it is subjected to higher temperatures. Moreover, in the event of an incident with the laser, if the temperature exceeds 200°C for more than 10 minutes or 180°C for more than 100 minutes, corrective actions should be taken and the adhesive should be replaced. These models therefore provide fundamental information for laser applications and will allow the implementation of preventive solutions during use but also in case of incident. Replacing the damaged adhesive sbmitted to thermal stresses will prevent damage to other components of the laser assembly. Replacing the damaged adhesive will prevent damage to other components of the laser assembly.

An important aspect of the targeted application that is not addressed yet is the exposure to laser radiation. Indeed, these adhesives are intended to coat optical fibers of high-power lasers and it is not to be excluded that the radiation can accelerate their degradation in addition to thermal oxidation.

6 Annex

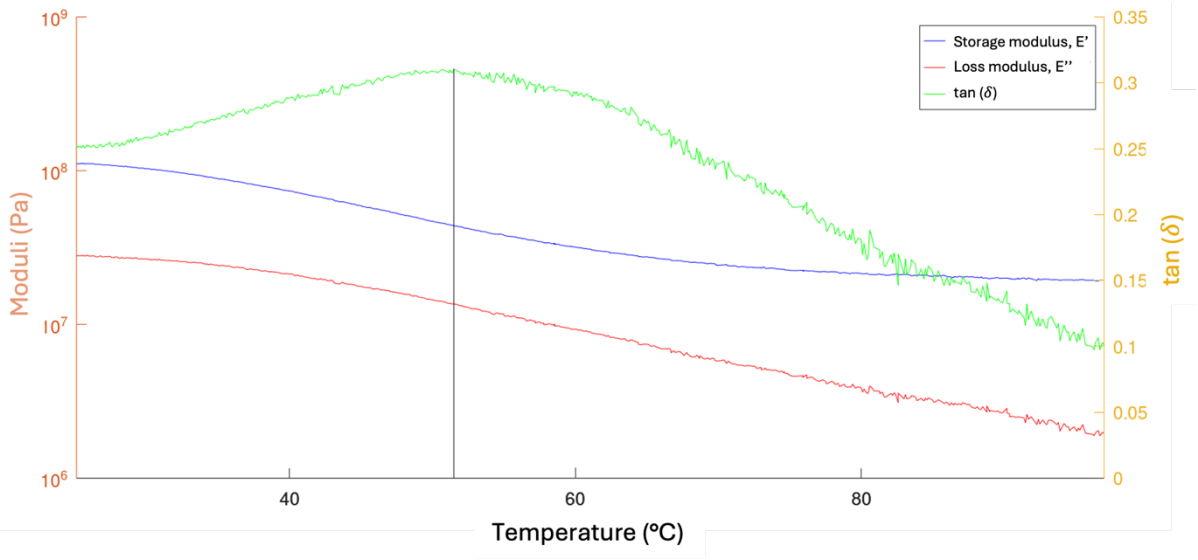

Figure 8: DMA curves of a PC373HA specimen in 10 mm 3-point bending. Deformation of 5µm at 1 Hz with a temperature ramp of 3°C/min.

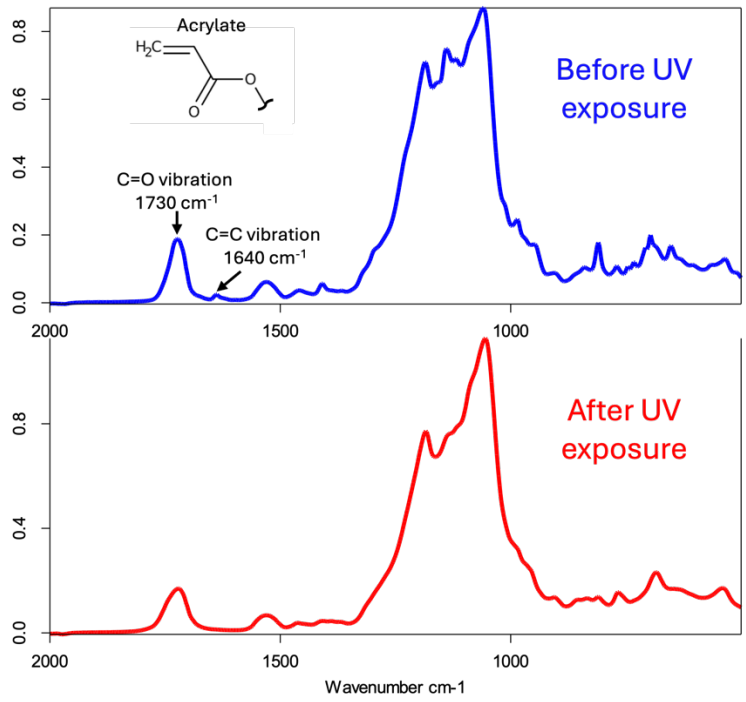

Figure 9: Infrared spectrum of the PC373HA resin before and after UV exposure (Spectra were recorded on a Bruker-VERTEX 70 instrument (400 to 4000 cm^{-1}, 4 cm^{-1} resolution, 32 scans, DLaTGS MIR) equipped with a Pike GladiATR optical design diamond crystal) for attenuated total reflectance (ATR).)

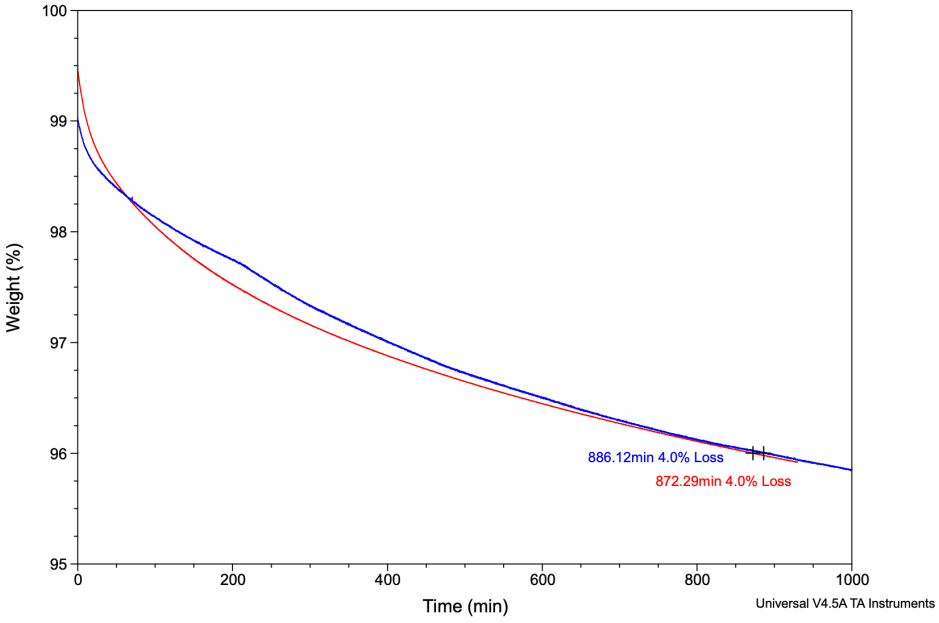

Figure 10: PC373HA isothermal TGA curves for a duration of 1000 min with an airflow rate of 60mL/min, at 150 °C. Repetition of the experiment.

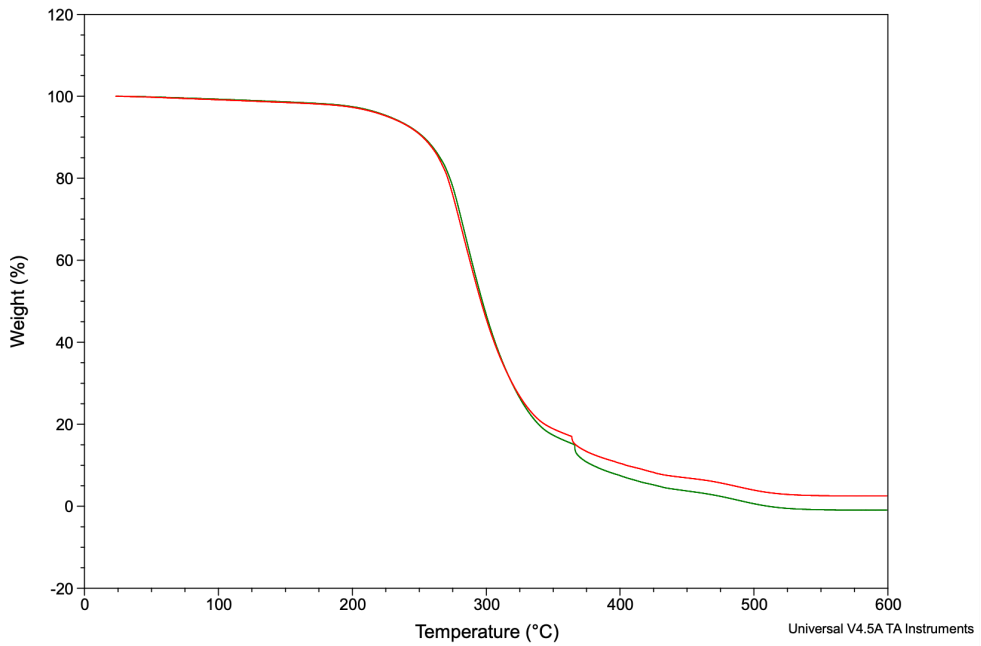

Figure 11: PC373HA TGA curves at 2 °C.min^{-1} with a 60 mL/min airflow rate. Repetition of the experiment.

7 References

[1] B. G. Yacobi, S. Martin, K. Davis, A. Hudson, and M. Hubert, Adhesive bonding in microelectronics and photonics, Journal of Applied Physics 91, 6227 (2002).

[2] Richard A Pethrick, Design and ageing of adhesives for structural adhesive bonding – A review, Proceedings of the Institution of Mechanical Engineers, Part L: Journal of Materials: Design and Applications, Volume 29, Issue 5, 2014.

[3] Adin, Hamit and Temiz, Şemsettin. "Experimental and Numerical Strength Analysis of Double Lap Joints Subjected to Tensile Loads" Materials Testing, vol. 56, no. 2, 2014, pp. 160-168. https://doi.org/10.3139/120.110521

[4] Adin, Hamit. "Effect of overlap length and scarf angle on the mechanical properties of different adhesive joints subjected to tensile loads" Materials Testing, vol. 59, no. 6, 2017, pp. 536-546. https://doi.org/10.3139/120.111031

[5] Rachid, H. B., Noureddine, D., Benali, B., & Adin, M. Ş. (2023). Effect of nanocomposites rate on the crack propagation in the adhesive of single lap joint subjected to tension. Mechanics of Advanced Materials and Structures, 1–9. https://doi.org/10.1080/15376494.2023.2240319

[6] Xiaoliang Zhou, Jialin Chen, Yuhang Li, Yuxin Sun and Yufeng Xing, Thermal tuning on band gaps of 2D phononic crystals considering adhesive layers, Journal of Physics D: Applied Physics, 51 075105

[7] LFM da Silva, A Pirondi, A Öchsner. Hybrid adhesive joints, Heidelberg: Springer, 2011

[8] L.C.E. Struik, Physical aging in plastics and other glassy materials, Polym. Eng. Sci., 17 (1977), pp. 165-173, 10.1002/pen.760170305

[9] L.C.E. Struik, Physical aging in amorphous glassy polymers, Ann. N. Y. Acad. Sci., 279 (1976), pp. 78-85, 10.1111/j.1749-6632.1976.tb39695.x

[10] E.C.L. Struik, Physical aging in amorphous polymers and other materials, PhD thesis, Delft university, 1977.

[11] Van Krevelen, D.W., Properties of Polymers: Their Correlation with Chemical Structure; their Numerical Estimation and Prediction from Additive Group Contributions: Fourth Edition, (2009), Elsevier Ed. pp. 1-1004. ISBN: 978-008054819-7

[12] Maamar F, Boudjemai A. Optomechanical optimal design configuration and analysis of glue pad bonds in lens mounting for space application. URL: Adv Space Res 2020;65(10):2263–75. https://doi.org/10.1016/j.asr.2020.01.025. 10.1016/j.asr.2020.01.025

[13] Jian Xiong, Zhijing Zhang, Xin Jin, Weimin Zhang, Theoretical modeling and calculation of stress fields in precision optical lens subjected to multi-point adhesive bonding assembly. Precision Engineering 73 (2022) 257–269

[14] Jon Harald L. Grave, Magnus L. Håheim, Andreas T. Echtermeyer, Measuring changing strain fields in composites with Distributed Fiber-Optic Sensing using the optical backscatter reflectometer, Composites Part B: Engineering, Volume 74, 1 June 2015, Pages 138-146

[15] Lee, Seunglok; Park, Jeewon; Ma, Hayoung; Kim, Wonjun; Song, Young Kyu; Lee, Dong Woog; et al. (2024). Multifunctional Acrylic Polymers with Enhanced Adhesive Property Serving as Excellent Edge Encapsulant for Stable Optoelectronic Devices. ACS Publications. Collection. https://doi.org/10.1021/acsami.3c16598

[16] R. Khaleghi Qusheh Bolagh, A. Salimi, K. Kabiri, A. Pourali, Synthesis and evaluation of novel aromatic acrylic monomers for optically clear adhesive with high refractive index, J. Appl. Polym. Sci. 2023, 140(4), e53375. https://doi.org/10.1002/app.53375

[17] Chloé Landreau, Adriana Morana, Nicolas Ponthus, Thomas Le Gall, Jacques Charvin, et al.. Influence of Adhesive Bonding on the Dynamic and Static Strain Transfers of Fibre Optic Sensors. Photonics, 2023, 10 (9), pp.996. ⟨10.3390/photonics10090996⟩. ⟨hal-04253190⟩

[18] Lin X, Yan H, Ma Y, Zhou Z. A construction method of the quasi-monolithic compact interferometer based on UV-adhesive bonding. Rev Sci Instrum. 2023 Jul 1;94(7):074501. doi: 10.1063/5.0155637. PMID: 37470703.

[19] B.Q. Yan, X.L. Zhang, S.Y. Guo, Rapid ultraviolet curing of epoxy acrylate films with low refractive index and strong interfacial adhesion, React. Funct. Polym., 178 (2022), Article 105356. https://doi.org/10.1016/j.reactfunctpolym.2022.105356.

[20] R. Paschotta, article on 'fiber cladding' in the *Encyclopedia of Laser Physics and Technology*, 1. edition October 2008, Wiley-VCH, ISBN 978-3-527-40828-3

[21] Engeldinger H.K., Lim C.R. (2011) Storage of Adhesives. In: da Silva L.F.M., Öchsner A., Adams R.D. (eds) Handbook of Adhesion Technology. Springer, Berlin, Heidelberg.

[22] Gibran da Cunha Vasconcelosa, Rogério Lago Mazura, Bruno Ribeiroa, Edson Coccieri Botelhoa, Michelle Leali Costa, Evaluation of Decomposition Kinetics of Poly (Ether-Ether-Ketone) by Thermogravimetric Analysis, Materials Research. 2014; 17(1): 227-235

[23] Křižanovský, L. and Václav Mentlík. “The use of thermal analysis to predict the thermal life of organic electrical insulating materials.” Journal of thermal analysis 13 (1978): 571-580.

[24] Nguyen, L.H. and Gu, M. (2005), Decomposition Kinetics, Life Estimation, and Dielectric Study of an Acrylate based Photopolymer for Microfabrication and Photonic Applications. Macromol. Chem. Phys., 206: 1659-1664.

[25] Plota, A.; Masek, A. Lifetime Prediction Methods for Degradable Polymeric Materials—A Short Review. *Materials* **2020**, *13*, 4507.

[26] Cui, HW., Jiu, JT., Sugahara, T. et al. Using the Friedman method to study the thermal degradation kinetics of photonically cured electrically conductive adhesives. J Therm Anal Calorim 119, 425–433 (2015). https://doi.org/10.1007/s10973-014-4195-3

[27] Brown M 2001 Introduction to thermal analysis: techniques and applications (Netherlands: springer)

[28] Marleine Morcos, Georges Challita, Vincent Legrand, Khaled Khalil, Pascal Casari, Impact strength of thermally aged double lap adhesively bonded joints, International Journal of Adhesion & Adhesives 112 (2022) 103029
[29] Eko Setio Wibowo, Sukma Surya Kusumah, Subyakto, Kenji Umemura, Modification of novel bio-based adhesive made from citric acid and sucrose by ZnCl2, International Journal of Adhesion & Adhesives 108 (2021) 102866

[30] Sevda Boran Torun, Investigation of the properties of fiberboards made from microcrystalline cellulose and antimony trioxide added melamine formaldehyde adhesive, International Journal of Adhesion & Adhesives 113 (2022) 103084

[31] Hassan Charii, Abdelghani Boussetta, Anass Ait Benhamou, Mehdi Mennani, Kamal Essifi, El-Houssaine Ablouh, Henri EL Zakhem, Nabil Grimi, Khalid Boutoial, Amine Moubarik, Exploring the potential of chitin and chitosan extracted from shrimp shell waste in enhancing urea-formaldehyde wood adhesives, International Journal of Adhesion & Adhesives 129 (2024) 103599

[32] Amine Moubarik, FranciscoJ.Barba, NabilGrimi, Understanding the physicochemical properties of olive kernel to be used as a potential tool in the development of phenol-formaldehyde wood adhesive, International JournalofAdhesion&Adhesives61(2015)122–126

[33] Cho-Hee Park, Seung-Woo Lee, Ji-Won Park, Hyun-Joong Kim; Preparation and characterization of dual curable adhesives containing epoxy and acrylate functionalities. Reactive & Functional Polymers 73 (2013) 641–646

[34] Elena V. Bystritskaya, Tatyana V. Monakhova, Victor B. Ivanov, TGA application for optimising the accelerated aging conditions and predictions of thermal aging of rubber, Polymer Testing, Volume 32, Issue 2, 2013, Pages 197-201.

[35] Salla, J., Morancho, J., Ramis, X. et al. Isothermal degradation and thermooxidative degradation of an epoxy powder coating. J Therm Anal Calorim 80, 163–169 (2005). https://doi.org/10.1007/s10973-005-0630-9

[36] Sbirrazzuoli, N. Advanced Isoconversional Kinetic Analysis for the Elucidation of Complex Reaction Mechanisms: A New Method for the Identification of Rate-Limiting Steps. *Molecules* 2019, *24*, 1683

[37] Marques, E. A. S., da Silva, L. F. M., Banea, M. D., & Carbas, R. J. C. (2014). Adhesive Joints for Low- and High-Temperature Use: An Overview. The Journal of Adhesion, 91(7), 556–585. https://doi.org/10.1080/00218464.2014.943395